

INVESTIGATIONS ON KONUS BEAM DYNAMICS USING THE PRE-STRIPPER DRIFT TUBE LINAC AT GSI

C. Xiao*, X.N. Du, and L. Groening

GSI Helmholtzzentrum für Schwerionenforschung GmbH, D-64291 Darmstadt, Germany

Abstract

Interdigital H-mode (IH) drift tube linacs (DTLs) based on KONUS beam dynamics are very sensitive to the rf-phases and voltages at the gaps between tubes. In order to design these DTLs, a deep understanding of the underlying longitudinal beam dynamics is mandatory. The report presents tracking simulations along an IH-DTL using the PARTRAN and BEAMPATH codes together with MATHCAD and CST. Simulation results illustrate that the beam dynamics design of the pre-stripper IH-DTL at GSI is sensitive to slight deviations of rf-phase and gap voltages with impact to the mean beam energy at the DTL exit. Applying the existing geometrical design, rf-voltages, and rf-phases of the DTL were re-adjusted.

KONUS BEAM DYNAMICS DESIGN

A Hamiltonian can be constructed describing the longitudinal particle motion in phase space as

$$H = -\frac{\pi w^2}{\beta_s^3 \gamma_s^3 \lambda} - \frac{q E_{acc} T_n(\beta_r)}{mc^2} (\sin \psi_r - \psi_r \cos \psi_s), \quad (1)$$

since ψ and w are variables canonically dependant on s

$$\frac{d\psi}{ds} = -\frac{2\pi w}{\beta_s^3 \gamma_s^3 \lambda}, \quad \frac{dw}{ds} = \frac{q E_{acc} T_n(\beta_r)}{mc^2} (\cos \psi_r - \cos \psi_s), \quad (2)$$

where q is the electric charge, m is the mass of the particle, c is the velocity of light, λ is the rf-frequency, and γ_s is the relativistic gamma factor. ψ_r is the phase of the field when the particle is at gap center, ψ_s is the synchronous phase, E_{acc} is the accelerating gradient, and T is the transient time factor. The subscripts s and n refer to the synchronous particle and the cell number, respectively. The energy gain of a particle may be expressed through the difference of its individual phase to the synchronous phase. For simplicity this term is normalized to the rest energy of the particle under study, suggesting the substitution

$$w = \frac{W_n - W_{n,s}}{mc^2}. \quad (3)$$

In conventional longitudinal beam dynamics the reference particle and the synchronous particle are identical. Longitudinal focusing is obtained by operating at constant negative rf-phase, such that the reference particle passes the gap center before the crest of the cosine-like gap voltage is reached. In conventional linacs the reference particle with design rf-phase of 0° (on rf-crest) will have maximum energy gain, but

the rf-phase range for stable longitudinal motion vanishes implying longitudinal acceptance of size zero.

In KONUS the reference particle and the synchronous particle are not the same. The gap-to-gap spacings are adjusted such that the synchronous particle arrives at 0° at each gap center. The beam is injected into a KONUS section such that the energy of the reference particle is higher than the synchronous particle energy. Additionally, the rf-phase of the reference particle at the first gap is close to the 0° synchronous phase. As the particle advances from gap to gap, the reference particle position will move counter clockwise in the longitudinal phase space diagram as illustrated in Fig. 1.

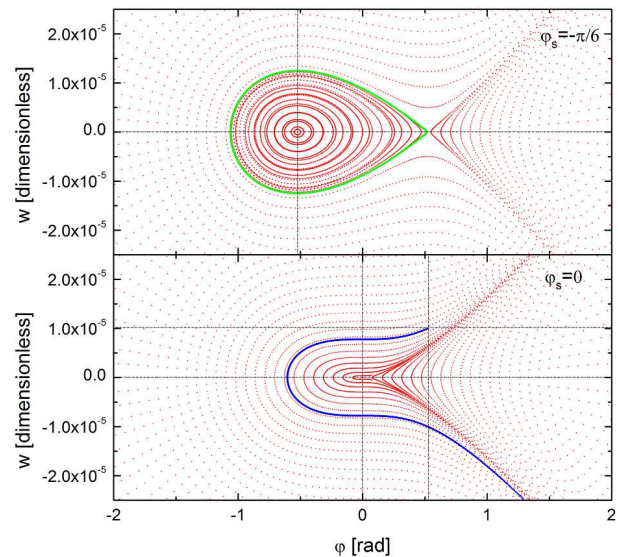


Figure 1: Conventional negative phase structure (upper) and KONUS structure (lower). In conventional designs, the rf-phase of the synchronous (reference) particle is always constant and negative ($\psi_s \approx -30^\circ$). Its energy is equal to the design energy ($w=0$). In KONUS the rf-phase and the energy difference of the reference particle w.r.t. the synchronous particle vary. The reference particle motion is not stable (blue line).

The parameters of the IH-DTL used as a reference in the following are listed in Table 1. This DTL provides transverse and longitudinal beam focusing for a long H-mode linac section, where the defocusing effects of transverse rf-fields and space-charge must be compensated avoiding quadrupole focusing lenses in each drift tube.

Almost all DTLs based on KONUS have been designed with LORASR [1]. One main feature of this code is provision of the gap field map. It builds the field map from

* c.xiao@gsi.de

Table 1: GSI Pre-Stripper IH-DTL Parameter List

Parameter	Value
Frequency	36.136 MHz
Design particle	$^{238}\text{U}^{4+}$
Design intensity	15 emA (electric)
Energy range	0.12 to 1.4 MeV/u
Number of cavities	2
Total length	20 m
Number of sections	4(IH-1)+ 2(IH-2)
Norm. exit rms-emittances	0.1 mm-mrad, 0.45 keV/u-ns

the geometry of gaps and drift tubes and the field map is stored in the code. The front half tube length is assumed equal to the end half tube length. This assumption is not strictly justified as the drift tube lengths increase along the DTL. On-axis longitudinal field distributions for ten types of gap and drift tube geometries are pre-calculated and stored, propagation of single particle coordinates is performed in thirty steps per gap by LORASR.

As input for LORASR the effective voltage and rf-phase at each gap n , $U_{eff,n}$ and ψ_n are used. The energy gain along gap n is calculated as

$$W_{n+1} - W_n = qU_{eff,n} \cos \psi_n, \quad (4)$$

$$U_{eff,n} = U_n T_n, \quad (5)$$

where ψ_n is the reference particle rf-phase at cell number n and U_n is the time dependent voltage between tubes of cell number n . From the given effective voltages and rf-phases LORASR calculates the according lengths of tubes and gaps, i.e., the DTL geometry. Additionally, the corresponding reference particle energies are provided at the exit of each cell.

The beam dynamics design of the UNILAC high current injector (HSI) was done at the IAP of the Goethe University of Frankfurt. According to KONUS beam dynamics, a section is defined as a set of gaps having the same synchronous particle definition. As a consequence each new section comes along with the re-definition of the synchronous particle (usually a transition from 0° to negative synchronous phase, -30° for instance, and vice versa). A complete IH-cavity can comprise one or several sections. The HSI is divided into two IH-cavities. The first cavity, IH-1, contains four sections while IH-2 contains two sections.

The effective gap voltages and the rf-phases serve as input for LORASR. The transient time factors (TTF) of DTL cells are calculated by LORASR and treated as constant values. After the IH-DTL was assembled the real gap voltage distribution along the two cavities has been measured and the measured gap voltages slightly (few percent) differed from the values being initially used for the beam dynamics design [2].

Using measured gap voltages instead of those used for the design, effects the single energy gains after each single cell and in turn the phases along subsequent cells. LORASR neglects this phase deviations in assuming that the phases

remain unchanged. Although the difference between measured and assumed gap voltages are quite small, the large amount of subsequent and phase-locked cells along an accelerating cavity leads to an accumulation of phase deviations and hence to output energy deviation.

Figure 2 shows the longitudinal focusing being simulated with LORASR using measured voltages and designed rf-phases. The initial energy of the reference particle was defined 0.1200 MeV/u, and the final energy of the reference particle was calculated as 1.3837 MeV/u applying Equ. 4. In the pre-stripper IH-DTL design, the longitudinal focussing initially simulated with LORASR is referred to as scenario-0.

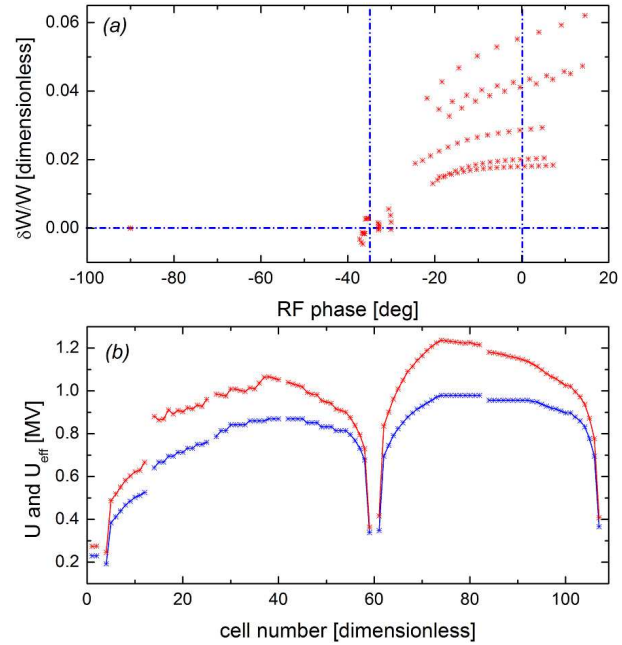


Figure 2: (a): Longitudinal reference particle position at each gap along the KONUS period. Red dots refer to the reference particle. (b): Measured voltage (red) and corresponding effective voltage (blue) at each gap along the IH-DTL (scenario-0).

SINGLE-PARTICLE TRACKING

In the following an estimate of the parameter set ($U_{eff,n}$, ψ_n , and w_n) is performed w.r.t. self consistency of effective gap voltages, rf-phases, and energies by applying the analytical method of Equ. 4. The rf-phase of the reference particle at the subsequent gap $n + 1$ is calculated straightforward. The augmented energy is the previous n_{th} cell's reference energy plus the energy gain across the gap. Each cell is represented as drift-gap-drift (see Fig. 3) and the rf-phase shift across the cell is determined by the distance between two gaps $L_{n,n+1}$ and the particle velocity β_{n+1}

$$\psi_{n+1} - \psi_n = \frac{2\pi L_{n,n+1}}{\beta_{n+1} \lambda} - \pi, \quad (6)$$

where $L_{n,n+1}$ is the distance between gaps n and $n + 1$,

Content from this work may be used under the terms of the CC BY 3.0 licence (© 2018). Any distribution of this work must maintain attribution to the author(s), title of the work, publisher, and DOI.

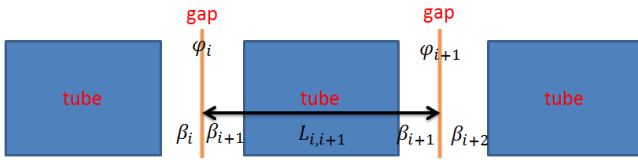


Figure 3: Definition of DTL cell and rf-phase along a drift-gap-drift sequence.

and β_{n+1} is the particle velocity between the gaps. The calculation of the transit time factor T_n by this analytical calculation assumes constant velocity between centers of adjacent gaps. Accordingly, smooth acceleration within the gap is approximated by a instantaneous step of particle velocity at the gap center.

In contrast to LORASR the BEAMPATH [3] code can use external two-dimensional field maps and simulate DTLs applying a consistent procedure. Rf-phases of the reference particle along the DTL are not assigned (except at the entrance gap) but rather calculated from the cell lengths and potential differences between tubes. Phase errors from preceding cells are thus propagated.

In the first simulation, the measured gap voltages from LORASR were taken for input. Initial rf-phases of buncher, IH-1, and IH-2 are chosen in order to ensure that the phases of the reference particle at the first gap of buncher, IH-1, and IH-2 are equal to the values put into LORASR: -90.0° , 14.5° , and 36.7° , respectively. All gap phases of the reference particle obtained from BEAMPATH together with the defined voltages are defined as scenario-1, and they are plotted in Fig. 4 together with the corresponding values from scenario-0.

It is re-iterated that scenario-0 is on the results from LORASR using as input phases and voltages at each single gap. Scenario-1 comprises results from BEAMPATH using as input the same gap voltages as scenario-0 but using just the first gap phase as input identical to scenario-0. In scenario-1 BEAMPATH calculates subsequent gap phases in a self-consistent way rather than using pre-defined values.

Phases of the reference particle are in good agreement along the buncher and the first section of IH-1. However, the phases differ significantly when the reference particle enters into the second section of IH-1 and in the following sections the phases delivered by LORASR and BEAMPATH remain being different. When the particles enters into IH-2 a the phase at its first gap is re-adjusted. In order to judge which result is more reliable, a dedicated routine based on MATHCAD has been established and applied.

In MATHCAD [4], the axially symmetric electric field map inside a gap is described by Fourier-Bessel series (the same as BEAMPATH). The reference particle vector function is defined as [5]

$$Z(t, z) := \begin{bmatrix} z \\ \frac{dz}{dt} \end{bmatrix} = \begin{bmatrix} z \\ \beta c \end{bmatrix}, \quad (7)$$

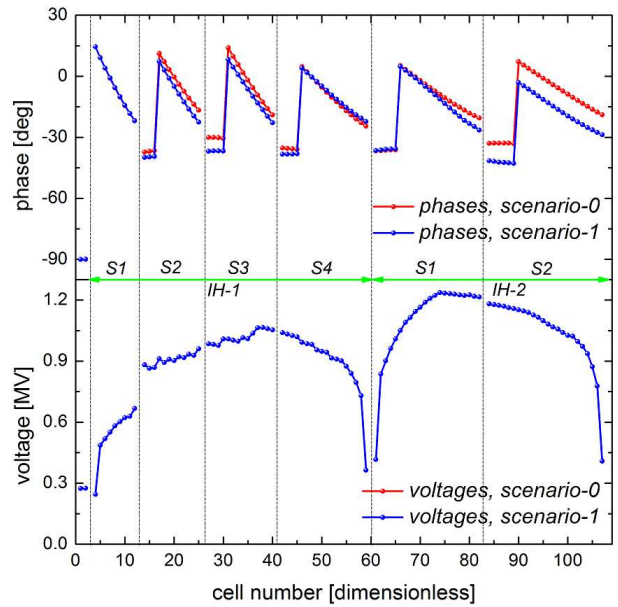


Figure 4: Comparison of scenario-0 and scenario-1. Upper: Rf-phases of the reference particle obtained from LORASR (red) and BEAMPATH (blue) simulations. Lower: Gap voltages used for LORASR (red) and BEAMPATH (blue) simulations (gap voltages are identical for both scenarios).

with βc as velocity. Starting at $t=0$ and $z=0$ (here BEAMPATH is repeated)

$$Z(0, 0) := \begin{bmatrix} 0 \\ \beta_0 c \end{bmatrix}. \quad (8)$$

The derivative DZ is

$$DZ(t, z) := \frac{dZ(t, z)}{dt} = \begin{bmatrix} \beta c \\ \frac{q}{m_0} E_z(z) \cos(\omega t + \psi_0) \end{bmatrix}. \quad (9)$$

This differential equation is non-linear and cannot be solved analytically. MATHCAD provides several routines to solve systems of ordinary differential equations. Each one uses a different integration algorithm and takes the same arguments. The Bulirsch-Stoer method (a very robust method which some prefer over Runge-Kutta) is applied solving Equ. 9 and the results are written as matrix F

$$F = \text{Bulstoer}[Z(0,0), t_i, t_f, s, DZ(t, z)], \quad (10)$$

where $Z(0,0)$ is the vector with initial conditions, t_i and t_f are the starting and ending points of the integration, s is the number of integration steps, and $DZ(t, z)$ is the vector containing the differential equations. At each step

$$F^1 = t_n, F^2 = z_n, F^3 = \beta_n c, \quad n = 1, 2 \dots s. \quad (11)$$

$F^{1,2,3}$ indicates F matrix columns 1, 2, and 3. LORASR output provides rf-phases at the center of each gap and energies at the centers of each tube ($E_z=0$ positions). BEAMPATH outputs the phases and energies at the center of each gap and

hence it is hard comparing energy gains directly between LORASR and BEAMPATH. Therefore, velocity gains from one tube center to the subsequent tube center are compared between LORASR and MATHCAD, and velocity gains from one gap center to the subsequent gap center are compared between BEAMPATH and MATHCAD as shown in Fig. 5.

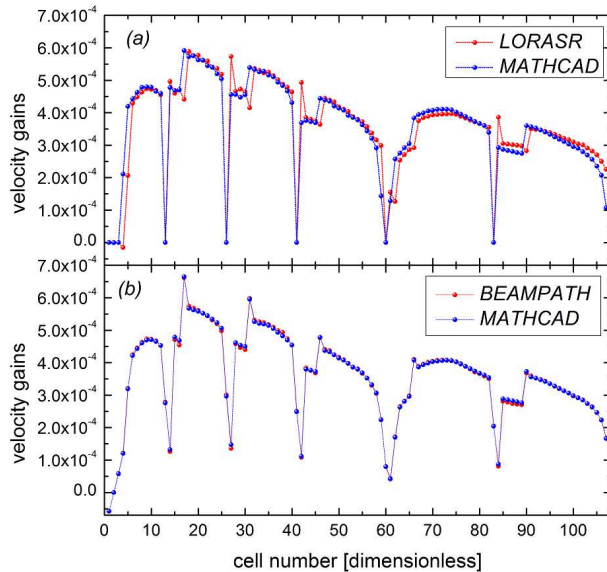


Figure 5: (a): Velocity gains from tube center to following tube center using LORASR and MATHCAD. (b): Velocity gains from gap center to following gap center using BEAMPATH and MATHCAD.

It is concluded that MATHCAD and BEAMPATH deliver quite similar phases at the gap centers and that the calculated velocity gains between gap centers are almost identical. Compared with results from LORASR, simulations with BEAMPATH deliver more reliable results. For the next set of simulations, gap voltages along each cavity and the initial rf-phase of IH-2 are slightly tuned in order to obtain similar phases as provided from LORASR. Gap voltages of the buncher, IH-1, and IH-2 have been multiplied by factors of 1.00, 0.985, and 0.975. Initial phases of the buncher and IH-1 are kept at -48.8° and 105.1° . But the initial phase of IH-2 has been re-changed to 152.4° . Corresponding phases and gap voltages obtained from BEAMPATH simulation are defined as scenario-2 and are plotted in Fig. 6 together with results from scenario-0.

It can be summarized that according to results of single particle tracking using BEAMPATH based on the existing HSI-DTL geometry, rf-phases of the reference particle using gap voltages as assumed in LORASR cannot be fully reproduced.

The final energies of the reference particle were calculated as 1.3837 MeV/u using scenario-0 (LORASR), 1.3992 MeV/u using scenario-1 (BEAMPATH), and 1.4010 MeV/u using scenario-2 (BEAMPATH), respectively.

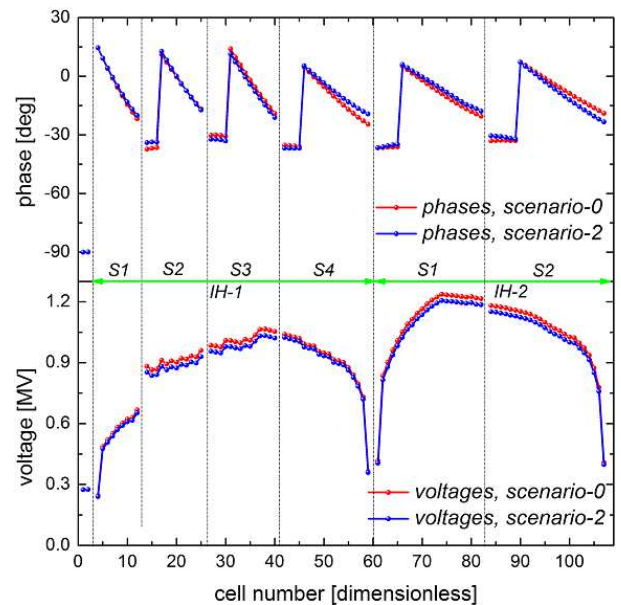


Figure 6: Comparison of scenario-0 and scenario-2. Upper: Rf-phases of the reference particle obtained from LORASR (red) and BEAMPATH (blue) simulations. Lower: Gap voltages used for LORASR (red) and BEAMPATH (blue) simulations.

MULTI-PARTICLE TRACKING

An artificial beam is assumed at the entrance of the MEBT in front of the IH-DTL being captured by the two-gaps buncher. This beam's macro-particles are set on the beam axis, i.e., $x=y=0$, $x'=y'=0$. Longitudinal particle distributions at the entrance and the exit of the MEBT simulated with MATHCAD are shown in Fig. 7.

For the case of the two-gaps buncher with identical gap voltages and initial rf-phases, the particle distributions at $T=14$ applying field-maps of CST and BEAMPATH ($M=1$ and $M=30$) are very similar. In other word, field-maps generated from BEAMPATH are sufficient to simulate the beam dynamics through the rf-gaps.

In the following multi-particle tracking simulations of BEAMPATH, $M=30$ is adopted. In the following simulations along the whole IH-DTL with BEAMPATH and PARTRAN [6] are compared to check and to modify the longitudinal beam dynamics of the HSI-DTL. PARTRAN is a z-code and each DTL cell uses a sequence of quadrupole, drift, and non-linear thin lens to model longitudinal and transverse rf-kicks at the electrical center of each DTL cell. PARTRAN uses pre-calculated TTF.

For further cross-checking between PARTRAN and BEAMPATH, in the following just the self-consistent scenario-2 is focused on. The time transition factor TTF, rf-phase, and effective voltages of each cell are complicated functions of both the field distribution and reference particle velocity, which may change appreciably during the passage through the multiple gap cavity. Another dedicated subroutine based on MATHCAD has been developed to solve these

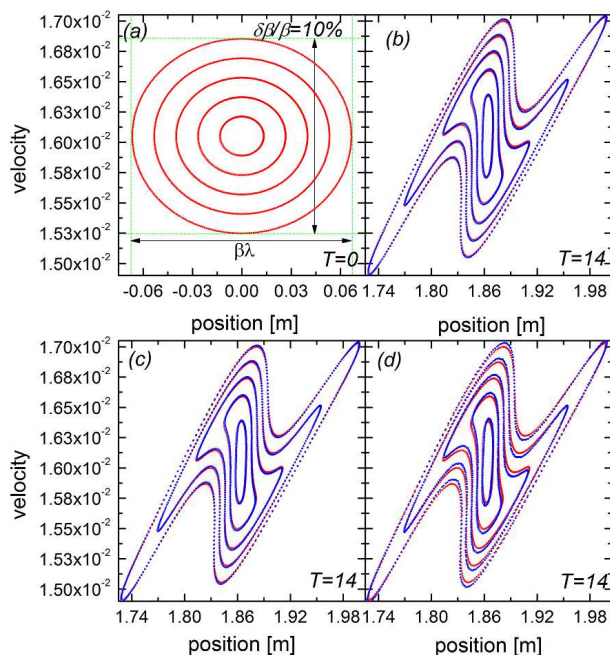


Figure 7: (a): Longitudinal particle distributions at time $T=0$ in scale of one rf-period. (b) and (c): Simulated longitudinal particle distributions at time $T=14$, red dots indicate results using actual longitudinal electric field calculated from CST, and blue dots indicate results using analytical longitudinal electric fields calculated from BEAMPATH ((b): $M=1$ and (c): $M=30$). (d): Simulated longitudinal particle distributions at the time of $T=14$, red dots indicate results using actual longitudinal electric field calculated from CST, and blue dots indicate results using analytical rectangular electric field.

parameters from electrical field map of BEAMPATH simulation for self-consistent scenario-2. Then corresponding effective voltages, rf-phases, and TTF values served as input for PARTRAN simulation. This continuous beam with zero momentum spread is further transported and accelerated through the completed DTL and the resulting longitudinal distributions at its exit are displayed in Fig. 8.

Particle distributions obtained from PARTRAN using scenario-0 and from BEAMPATH using scenario-1 are significantly different, thus indicating significantly different longitudinal beam dynamics. Particle distributions from PARTRAN and BEAMPATH using scenario-2 are not exactly identical but quite similar, thus indicating highly similar longitudinal beam dynamics.

CONCLUSION

As in KONUS beam dynamics the reference particle (bunch center) is not identical to the synchronous particle, the reference particle moves around the synchronous particle in longitudinal phase space. The shift of rf-phase between subsequent gaps (given by the length of drift between them) is used by the designer to adjust the phase relation between the reference particle and the synchronous particle. This

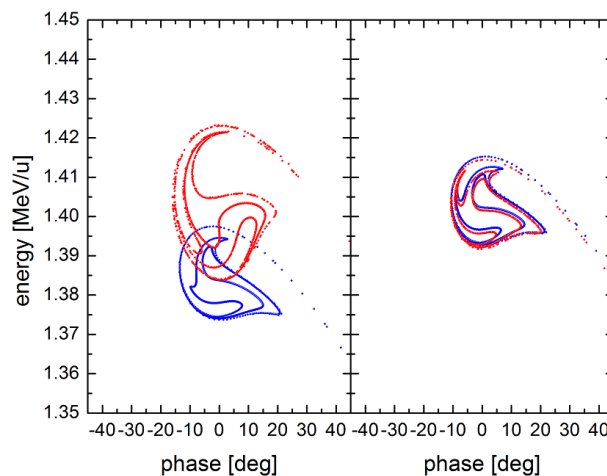


Figure 8: Longitudinal particle distributions at the exit of the DTL. Left: Results simulated from PARTRAN using scenario-0 (blue) and BEAMPATH using scenario-1 (red). Right: Results from PARTRAN (blue) and BEAMPATH (red) using scenarios-2.

adjustment takes place especially during the change of synchronous particle rf-phase from 0° to -30° and vice versa, i.e., during transition from one KONUS section into another. For cavities comprising many gaps small rf-phase errors being neglected may harm further stable acceleration along subsequent cavities and lower the precision of the predicted DTL output energy. The mentioned inconsistencies cannot be modelled by z -codes as PARTRAN for instance. Self-consistent beam dynamics of this IH-DTL optimized with the t -code BEAMPATH (scenario-2). These results could be reproduced very well with PARTRAN using realistic TTF parameters, measured gap voltages, and upgraded rf-phases taking into account unequal lengths of front and end half tubes.

REFERENCES

- [1] R. Tiede. LORASR code development. Proceedings of EPAC2006, Edinburgh, Scotland (2006).
- [2] B. Krietenstein et al. Numerical simulation and RF mode measurements of the new GSI IH-DTL. Particle Accelerator Conference 1997, vol. 2, pp. 2645-2647.
- [3] Y.K. Batygin. Particle-in-cell code BEAMPATH for beam dynamics simulations in linear accelerators and beamlines. Nuclear Instruments and Methods in Physics Research A 539 (2005) 455-489.
- [4] PTC Mathcad, <https://www.ptc.com/en/engineering-math-software/mathcad>
- [5] C. Xiao, X.N DU, and L. Groening. Investigations on KONUS beam dynamics using the pre-stripper drift tube linac at GSI. Nuclear Instruments and Methods in Physics Research A 887 (2018) 40-49
- [6] N. Pichoff, and D. Uriot. PARTRAN, Internal Memorandum, CEA, Saclay.

Content from this work may be used under the terms of the CC BY 3.0 licence (© 2018). Any distribution of this work must maintain attribution to the author(s), title of the work, publisher, and DOI.